

# Effect of Temperature on the Series and Shunt Resistance of a Silicon Solar Cell under Frequency Modulation

Gökhan Sahin

Electric and Electronic Engineering Department, IĞDIR University, Iğdır 76000, Turkey  
g.sahin38@hotmail.fr

**Abstract-**Temperature is a very important parameter that is often overlooked in the behavior of solar cells. This study presents the influence of temperature on the electrical parameters of a bifacial silicon solar cell under frequency modulation. Based on the equation of the continuity of the carriers, the expression of the density of the minority charge carriers, the photocurrent and the photo-voltage were determined. For all these temperatures the effect is interpreted as a function of frequency modulation. The aim of this work is to study the evolution of this density depending on temperature and its distribution in angular frequency and the junction recombination velocity in the bases for different values of the temperature.

**Keywords-** Photovoltaic; Junction Recombination Velocity; Angular Frequency; Series and Shunt Resistance; Temperature

## I. INTRODUCTION

The electric conversion of solar energy is obtained with semiconductor materials. The solar cell or photovoltaic cell is the basic element of a photovoltaic generator. It consists of a semiconductor material, generally silicon, that is treated by doping. Experience shows that the operation of solar cells strongly depends on several parameters, both internal (linked to the device itself) and external (related to the operation environment, irradiance, temperature, etc.) [1]. The temperature that is the subject of this study is an extremely important parameter and cannot be neglected in the behavior of solar cells. On this relatively large theme, we chose to study the effect of temperature applied in the base of a solar cell under polychromatic illumination. We limited this study to back side illumination. This is where the phenomenon of recombination velocity is very important. We looked at first of the influence of temperature on the minority carriers' density, then we are interested at effects on the photocurrent density and the photovoltage. About the study of I-V characteristic, we also looked for the effect of temperature and its distribution in angular frequency and junction recombination velocity on the series and shunt resistances.

## II. THEORY

This study is based on a bifacial silicon solar cell with an n+-p-p+ structure (Fig. 1) [1-3]. Given that the base has a greater contribution to the photocurrent, the following analyses have been conducted only in this region.



Fig. 1 Bifacial silicon solar cell

We assume a quasi-neutral p-type base, low injection condition and no lateral effect; the principal transport mechanism then remains the one-dimension diffusion of minority carriers (electrons). Carrier generation, recombination and drift/diffusion are the three major phenomena that occur inside the solar cell under illumination; in a steady state, the transport equation can be written as [3-6]:

$$D(\omega) \cdot \nabla^2 \delta(\omega, x, t) - \frac{\delta(\omega, x, t)}{\tau} + G(\omega, x, t) = \frac{\partial \delta(\omega, x, t)}{\partial t} \quad (1)$$

$\tau$  is the average lifetime of minority carrier's charge,  $G(\omega, x, t)$  is the global generation rate of carriers depending on the thickness  $x$ ,  $t$  is time and  $\delta$  is the density of photo created minority carriers.  $G(\omega, x, t)$  can be written as follows:

$$G(\omega, x, t) = \sum_{i=1}^3 na_i e^{(-b_i x)} e^{(j\omega t)} \quad (2)$$

$a_i$  and  $b_i$  are obtained from the tabulated values of the solar illumination spectrum and the dependence of the absorption coefficient of silicon with illumination wavelength, and  $n$  is the number of the sun.

$$\delta(x, t) = \delta(x) e^{(j\omega t)} \quad (3)$$

$\delta(x)$  is the density of picture minority charge carriers generated in the thickness  $x$  in the base. Replacing Eqs. (2) and (3) into (1), one obtains  $\delta(x)$ :

$$\frac{\partial^2 \delta(x)}{\partial x^2} - \frac{\delta(x)}{L^2} = - \frac{\sum_{i=1}^3 na_i e^{(-b_i x)}}{D} \quad (4)$$

$L$  is the diffusion length of excess minority carriers and  $D$  is the diffusion constant, which is related to the operating temperature through the relationship set forth in [7].

$$D = \mu \cdot \frac{kT}{q} \quad (5)$$

where  $q$  is the elementary charge,  $k$  is the boltzmann constant and  $T$  is the temperature.

$$n_i = A_n \cdot T^{\frac{3}{2}} \cdot \exp\left(\frac{Eg}{2KT}\right) \quad (6)$$

$n_i$  refers to the intrinsic concentration of minority carriers in the base [7],  $A_n$  is the specific constant of the material ( $A_n=3.87 \times 10^{16}$  for silicon) and  $N_b$  is the base doping concentration.

$$\tau = \frac{1}{C \cdot N_b} \quad (7)$$

$n(x)$  is respectively the excess minority carrier density,  $L$  is diffusion length,  $\tau$  is lifetime,  $\mu$  is mobility, and  $C$  is the proportionality coefficient. The solution of Eq. (4):

$$\delta(\omega, x, T) = A \cosh\left(\frac{x}{L}\right) + B \sinh\left(\frac{x}{L}\right) + n \sum \frac{L^2}{D} a_i e^{(-b_i x)} + \frac{L^2}{D} C \cdot A_n \cdot T^3 \cdot \exp\left(\frac{Eg}{KT}\right) \quad (8)$$

$A$  and  $B$  are constants that are determined by the two following boundary conditions:

- at the junction  $x=0$

$$\left. \frac{\partial \delta(\omega, x, T)}{\partial x} \right|_{x=0} = \frac{Sf}{D} \cdot \delta(\omega, 0, T) \quad (9)$$

This boundary condition introduces a parameter  $Sf$ , which is called the recombination velocity at the junction.  $Sf$  determines the charge carriers' flow through the junction and is directly related to the operating point of the solar cell [2-5]. The higher  $Sf$  is, the higher the current density will be.

- at the rear side  $x=H$

$$\left. \frac{\partial \delta(\omega, x, T)}{\partial x} \right|_{x=H} = \frac{Sb}{D} \cdot \delta(\omega, H, T) \quad (10)$$

Eq. (8) traduces the fact that the excess carrier concentration reaches its maximum value in the middle of the base due to the presence of junctions on both sides of the base along the  $x$  axis (Fig. 1).

A. Photocurrent Density

The photocurrent  $J_{ph}$  is obtained from the following equation, given that there is no drift current [2, 8].

$$J_{ph}(\omega, T, Sf) = q \cdot D \cdot \left. \frac{\partial \delta(\omega, x, T)}{\partial x} \right|_{x=0} \tag{11}$$

The figure below shows the photocurrent density as a function of the angular frequency for different values of the temperature.

B. Photovoltage

The photo-voltage is derived from the Boltzmann relation. The photovoltage can be expressed as [2, 8]

$$V_{ph}(\omega, T, Sf) = V_T \cdot \ln \left[ 1 + \frac{Nb}{n_0^2} \cdot \delta(\omega, T, Sf) \right] \tag{12}$$

where  $V_T$  is the thermal voltage,  $Nb$  is the base doping density ( $Nb=10^{16} \text{cm}^{-3}$ ),  $n_0$  is the intrinsic of minority carriers density in the base, and  $V_T(\omega, T, Sf) = \frac{K \cdot T}{q}$  is the thermal voltage.

C. Characteristic Current-Voltage

The characteristic current –voltage is represented by the following curve:

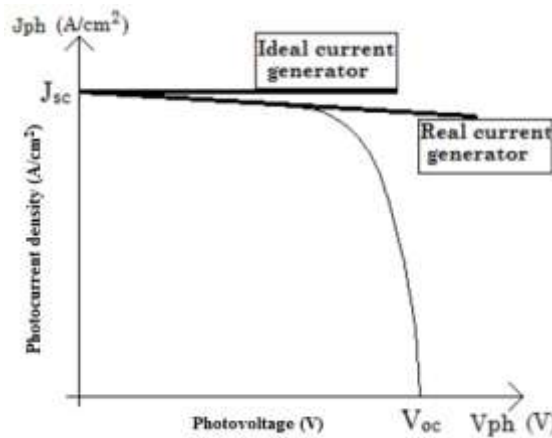


Fig. 2a Illuminated I-V curve

This characteristic presents two areas that are very important [9, 10]. Area 1 is has a current generator  $J_{sc}$  of admittance that can be modeled as  $\frac{1}{R_{sh}}$ .

The corresponding electrical circuit is:

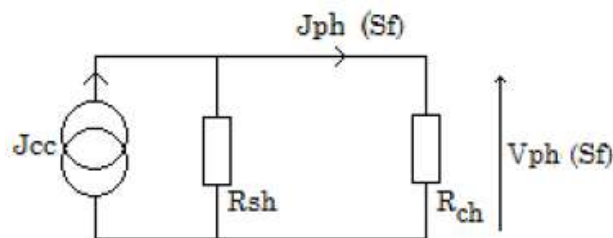


Fig. 2b Corresponding equivalent electrical circuit near short circuit

$J_{sc}$ : short circuit current density

$R_{sh}$ : shunt resistance per unit area

$J_{ph}$  et  $V_{ph}$ : density current and photovoltage

$R_{ch}$ : Load resistance

Fig. 2a shows that when the solar cell operates near the short circuit, which is for higher values of  $S_f$ , it behaves like a real current generator and therefore can be represented as an ideal current generator  $J_{sc}$  shunted by a parasitic resistance  $R_{sh}$ , as presented in Fig. 2b. Based on Fig. 2b, we can write that:

$$V_{ph}(\omega, T, S_f) = R_{sh} \cdot [J_{sc}(\omega, T, S_f) - J_{ph}(\omega, T, S_f)] \tag{13}$$

This equation can be rearranged, leading to an expression of the shunt resistance ( $R_{sh}$ ) in the form [10, 11]:

$$R_{sh}(\omega, T, S_f) = \frac{V_{ph}(\omega, T, S_f)}{J_{sc} - J_{ph}(\omega, T, S_f)} \tag{14}$$

Area 2 is similar to a generator voltage  $V_{oc}$  of equivalent resistance internal impedance  $R_s$  series. The model of an equivalent electrical circuit of a photocell operating in an open circuit is represented by the following Fig. 3a:

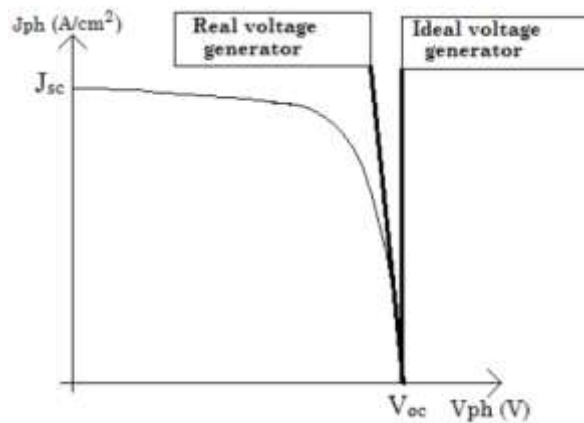


Fig. 3a Illuminated I-V curve

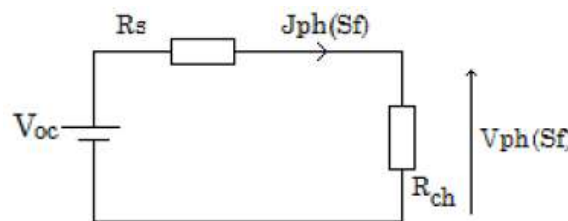


Fig. 3b Corresponding equivalent electrical circuit near short circuit

$V_{co}$ : Open circuit voltage

$R_s$ : Series resistance

$V_{ph}$ : Voltage

Applying the law of mesh to the circuit of Fig. 3a (area 2), since this expression has been determined near the short circuit, it holds only for high junction recombination velocity [10, 12] values.

On Fig. 3a, considering now that the solar cell operates near an open circuit. We can see on this I-V curve that it behaves like a real generator; thus, this corresponds to an ideal voltage generator in series with a parasitic resistance ( $R_s$ ) as presented in Fig. 3b. From the Kirchoff law applied to Fig. 3b, we have:

$$R_s(\omega, T, S_f) \cdot J_{ph}(\omega, T, S_f) = V_{oc} - V_{ph}(\omega, T, S_f) \tag{15}$$

Then, we deduce that:

$$R_s(\omega, T, S_f) = \frac{V_{co} - V_{ph}(\omega, T, S_f)}{J_{ph}(\omega, T, S_f)} \tag{16}$$

Contrary to Eq. (14), this above equation holds only for very low  $S_f$  values.

## III. RESULTS AND DISCUSSION

The two resistors model internal losses as follows [9, 10]:

- Series Resistance ( $R_s$ ): models the ohmic losses in the material.
- Shunts Resistance ( $R_{sh}$ ): models the parasitic currents traversing the cell.

We present the discussion of results based on simulations, applying the relations obtained from the current-voltage characteristics of a solar cell under polychromatic illumination in order to explore the effects of temperature on the electrical parameters of the device PV studied.

## A. Shunts Resistance

Fig. 4 shows the modulus of shunt resistance versus the logarithm of the modulation frequency for different values of the temperature.

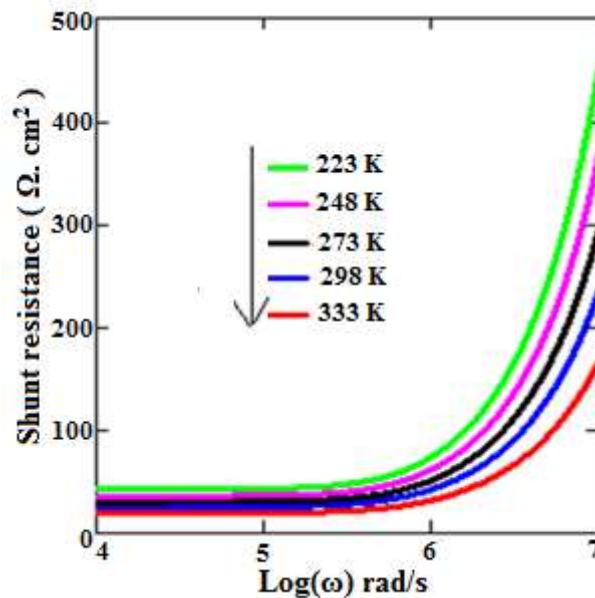


Fig. 4 Shunt resistance versus the logarithm of frequency  $\text{Log}(\omega)$  for different values of the temperature

Fig. 4 shows that the shunt resistance decreases with increasing temperature. The charge carrier's photo geneses under the effect of temperature. The temperature is equipped with great kinetic energy and puts them in a chaotic movement [13]. This random motion causes much collusion between the carriers and the leakage current. Thus, the diode current greatly increases. As a result, the shunt resistance decreases with increasing temperature.

From the curves in the figure, it can be seen that for a lower modulation frequency to about  $10^6 \text{ rad/s}$  the modulus of the shunt resistance varies weakly, but above this limit value, the shunt resistance increases rapidly with the modulation frequency.

We also note that the increase in temperature leads to a decrease of the amplitude of the shunt resistance. This behavior can be explained by the fact that the internal temperature of the material of the solar cell increases with solar energy and thereby the diffusion of carriers will be more significant on the solar cell as the temperature has an effect thermal stirrer. In addition, the temperature is at its maximum at the junction in a position of short circuit [14] since the junction is the focal point of the charge carriers photogenerated within the base of the solar cell. In fact, the presence of a large number of carriers in the base region near the junction results in a major source of higher temperatures. Like the density of minority charge carriers, the amplitude of the temperature is strongly influenced.  $R_{sh}$  is the shunt resistance.  $S_{fsc}$  is the junction recombination velocity initiating the short circuit.

Fig. 5 represents the shunt resistance versus logarithm of frequency  $\text{Log}(\omega)$  for various junction recombination velocity values:

Fig. 5 represents the profile of the Shunt Resistance ( $R_{sh}$ ) based on the recombination velocity at the junction for different values of the temperature. This figure shows that the shunt resistance is based on the junction recombination velocity. This increase of  $R_{sh}$  is all the more important when the temperature is low. Indeed, when the recombination velocity increases, many carriers arrive at the junction. Thus, these carriers cross the junction to participate in electric power. Thus, the leakage current is reduced: The variation of the shunt resistance module according to the logarithm of the frequency still shows an increase with the increasing frequency and also increases with the junction recombination velocity. When the junction recombination velocity increases, the flow of carriers across the junction also increases, and then there is a weakening of the

holders at the grassroots level, resulting in a dynamic conductivity reduction and increased shunt resistance.

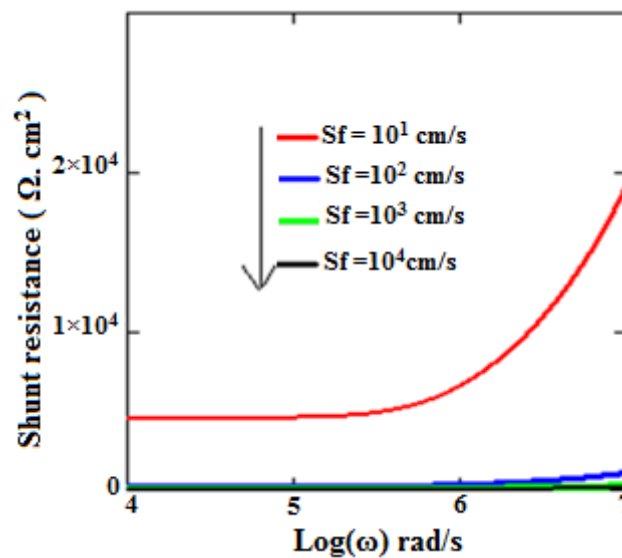


Fig. 5 Shunt resistance versus the logarithm of frequency for different values of the junction recombination velocity

### B. Phase of Shunt Resistance

The variation of the phase of the shunt resistor with the modulation frequency is shown in Fig. 6 below [12].

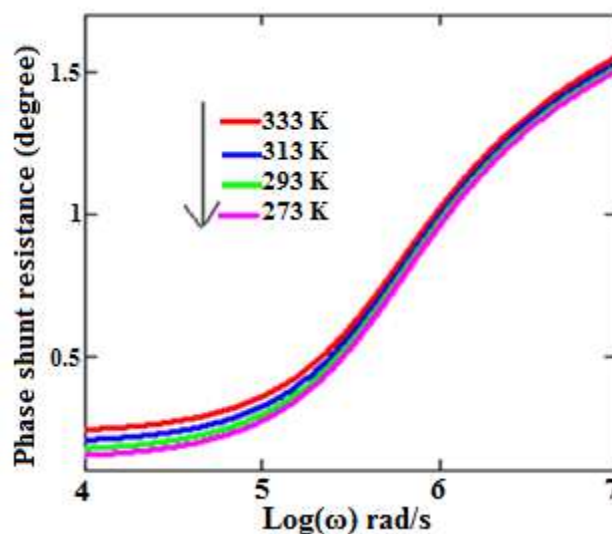


Fig. 6 Phase of the shunt resistance based on the modulation frequency for different values of the temperature

It can be seen that the phase of the shunt resistance increases with the increase of the modulation frequency. However, it is observed that the phase of the shunt resistor is always positive. Its horizontal junction solar cell has an inductive behavior, and this inductive reaction is greater for high values of data modulation frequency. We can say that when the modulation frequency is high, the response of the photocell is virtually zero. Very high frequencies block relaxation of the solar cell. It is seen that the temperature slightly increases the phase of the shunt resistor.

### C. Series Resistance

Fig. 7 illustrates the profile of the series resistance of the module as a function of the modulation frequency for different temperature values [14, 15].

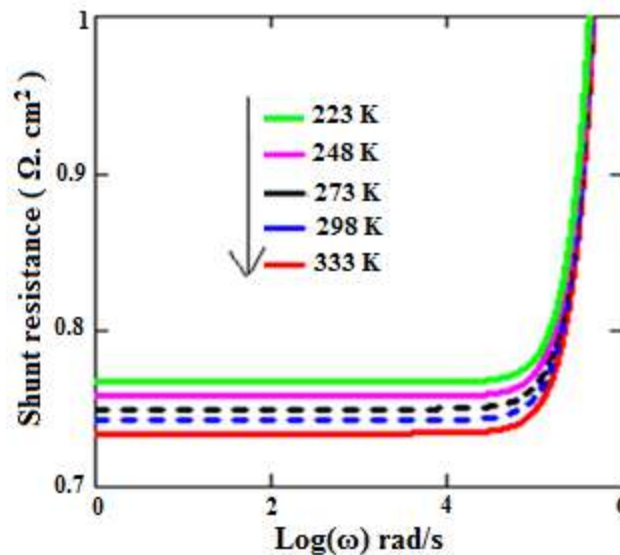


Fig. 7 Series resistance versus logarithmic angular frequency for various temperatures

Fig. 7 shows that the series resistance increases for the temperature. In fact, the increasing temperature creates a warming of a dilation of metals. This phenomenon increases the ability of materials to resist the passage of electric currents. Thus, a positive temperature gradient results in an increase in resistivity of semiconductor material; the constituent metal contacts the electrodes and the grid of the minority carrier collection. Fig. 8 below shows the series resistance of the module as a function of the modulation frequency for different junction recombination velocities. In the case of an open circuit [16] situation, the series resistance increases gradually with the junction recombination velocity. We also notice an increase of the series resistance with the logarithm of frequency. For determining the series resistance  $R_s$ , we propose the equivalent electrical model of the solar cell in an open circuit where the solar cell operates as a photovoltage generator associated with the series resistance and the temperature. For low values of the temperature, series resistance  $R_s$  is low and almost constant. The angular frequency causes an increase in series resistance. This increase in series resistance when the angular frequency increases is due to the fact that the blocking of the minority carriers within materials becomes significant due to the presence of angular frequency, which causes a reduction in the photocurrent. When the temperature increases, the series resistance decreases and this decrease is more marked for lower angular frequency values. Effectively, when the temperature increases, the impurity concentration increases also, leading to more and more recombination of excess minority carriers and then decrease of the series resistance.

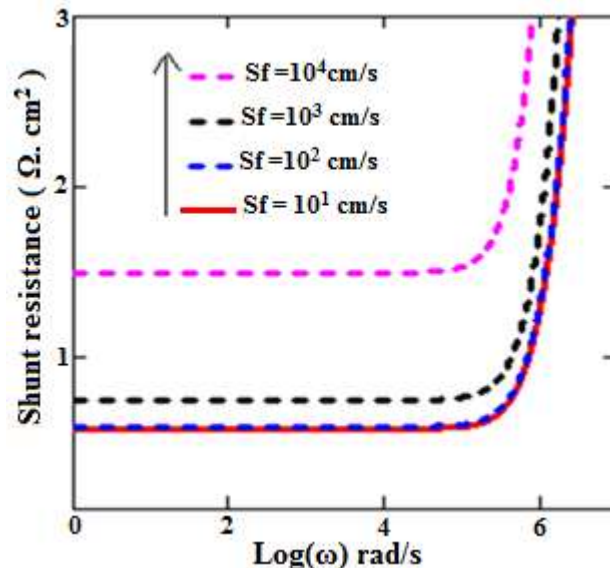


Fig. 8 Series resistance versus logarithmic angular frequency for various junction recombination velocities;  $z = 0.002$  cm

Fig. 8 represents the profile of the series resistance depending on the speed of recombination for different temperature values. This figure shows that the series resistance behaves on the basis of the recombination velocity at the junction. This increase of  $R_s$  is all the more important as the temperature rises. Indeed, when the recombination velocity increases, the diode characterizing the junction behaves as a resistance and opposes the passage of electric current [17].

It is also noted that the increase of  $S_f$  corresponding to an increase of the passage of electrons at the junction electron leads to a heating of the metal grids in the front and the back sides of the solar cell and increases the amplitude of the module. The series resistance varies exponentially with the modulation frequency, as observed.

#### D. Phase of the Series Resistance

The variation of the phase of the series resistance with the modulation frequency is shown in Fig. 9 [12].

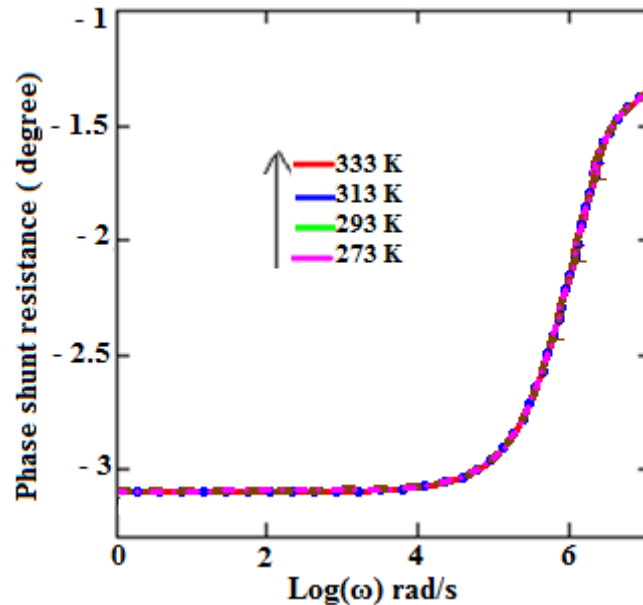


Fig. 9 Phase of the function series resistance of the modulation frequency for different values of the temperature

It is found that the variation of the phase of the series resistance is a function of the modulation frequency. Therefore, we see that the phase capacity is negative and the phases' effects outweigh the inductive. However, a slight variation of the phase occurs when the frequency is low of about  $10^4$  rad / s, but beyond this value there is a rapid increase in the series resistance phase. When the modulation frequency increases, the response of the photocell is very low. It is observed that the applied temperature slightly decreases the series resistance phase, which does not contribute to the good performance of the solar cell.

#### IV. CONCLUSIONS

In this theoretical study where the solar cell is enlightened at its back surface, we were able to highlight the influence of the temperature applied to the electrical parameters of the solar cell. From this study, we note that the back surface is very sensitive to temperature. The minority carrier's density increases with increasing temperature. The determination of the minority carrier's density in the base of the solar cell, led by expressions of the photocurrent and the photovoltage. This study was made according to logarithm of the frequency for various increasing temperature and junction recombination velocity values. This allowed us to establish the expressions of series and shunt resistances following two operating points (open-circuit situation and short-circuit situation), whose profiles were studied versus the logarithm of the frequency for various temperature and junction recombination velocity values. Also, we present a simulation study of a solar cell horizontal junction under polychromatic illumination in frequency modulation. Simulations show that the parasitic resistances (modulus and phase) are sensitive to the operating temperature, which is a very important parameter in the behavior of solar cells and the modulation frequency. It appears that whatever the temperature range, an increase in the target electrical parameters can be observed. The series resistance that characterizes the ohmic losses as smaller than the photocell is optimal. The shunt resistance ( $R_{sh}$ ) that characterizes the leakage current as greater than the photocell is optimal. It can be concluded that the increase in temperature in the material contributes significantly to the weakening of the performance of the photocell.

#### REFERENCES

- [1] J. Furlan and S. Amon, "Approximation of the carrier generation rate in illuminated silicon," *Solid State Electron.*, vol. 28, iss. 12, pp. 1241-1243, 1985.
- [2] D. Sontag, G. Hahn, P. Geiger, P. Fath, and E. Bucher, "Two-dimensional resolution of minority carrier diffusion constants in different silicon materials," *Solar Energy Materials & Solar cells*, vol. 72, iss. 1-4, pp. 533-539, 2002.
- [3] C. Schinke, D. Hinken, K. Bothe, C. Ulzhöfer, A. Milsted, J. Schmidt, and R. Brendel, "Determination of the Collection Diffusion Length by Electroluminescence," *Imaging Energy Procedia*, vol. 8, pp. 147-152, April 2011.
- [4] N. Nallusamy, S. Sampath, and R. Velraj, "Experimental investigation on a combined sensible and heat latent storage system integrated with constant/varying heat sources," *Renewable Energy*, vol. 32, iss. 7, pp. 1206-27, June 2007.

- [5] N. R. Vyshak and G. Jilani, "Numerical analysis of latent heat thermal energy storage system," *Energy Conver. Manag.*, vol. 48, iss. 21, pp. 61-68, June 2007.
- [6] A. Mandelis, "Coupled ac photocurrent and photothermal reflectance response theory of semiconducting p-n junctions," *Journal of Applied Physics*, vol. 66, iss. 11, pp. 5572-5583, 1989.
- [7] F. Agyenim, N. Hewitt, P. Eames, and M. Smyth, "A review of materials, heat transfer and phase change problem formulation for latent heat thermal energy storage systems (LHTESS)," *Renewable Sustainable Energy Rev.*, vol. 14, iss. 2, pp. 615-28, 2010.
- [8] J D Mondol, M Smyth, A Zacharopoulos, and T Hyde, "Experimental performance evaluation of a novel heat exchanger for a solar hot water storage system," *Appl. Energy*, vol. 86, iss. 9, pp. 1492-1505, 2009.
- [9] J Hu, H Dong, E Zhou, and W Yang, "Experimental study on heat charging performance of phase change thermal energy storage unit with helical coil," *ACTA Energiæ Solaris Sinica*, vol. 4, iss. 18, pp. 399-403, 2006.
- [10] B. Tripathi, P. Yadav, and M. Kumar, "Effect of Varying Illumination and Temperature on Steady-State and Dynamic Parameters of Dye-Sensitized Solar Cell Using AC Impedance Modeling," *Hindawi Publishing Corporation International Journal of Photoenergy*, Article ID 646407, 10 pages, July 2013.
- [11] G Sahin, "Effect of wavelength on the electrical parameters of a vertical parallel junction silicon solar cell illuminated by its rear side in frequency domain," *Results in Physics*, vol. 6, pp. 107-111, March 2016.
- [12] G Sahin, D Moustapha, A O E M Mohamed, I N Moussa, T Amary, and S Grégoire, "Capacitance of Vertical Parallel Junction Silicon Solar Cell under Monochromatic Modulated Illumination," *Journal of Applied Mathematics and Physics*, vol. 3, pp. 1536-1543, November 2015.
- [13] Y Sun, F Xu, G Yang, Y Shi, and L Ma, "Experimental Study on Thermal Discharge Performance of A Phase Change Thermal Storage Material," *The Open Materials Science Journal*, vol. 9, pp. 77-81, 2015.
- [14] K. Ocakoglu, F. Yakuphanoglu, J. R. Durrant, and S. Icli, "The effect of temperature on the charge transport and transient absorption properties of K27 sensitized DSSC," *Solar Energy Materials and Solar Cells*, vol. 92, no. 9, pp. 1047-1053, 2008.
- [15] D. Pysch, A. Mette, and S.W. Glunz, "A review and comparison of different methods to determine the series resistance of solar cells," *Solar Energy Materials and Solar Cells*, vol. 91, no. 18, pp. 1698-1706, 2007.
- [16] R. Kern, R. Sastrawan, J. Ferber, R. Stangl, and J. Luther, "Modeling and interpretation of electrical impedance spectra of dye solar cells operated under open-circuit conditions," *Electrochimica Acta*, vol. 47, no. 26, pp. 4213-4225, 2002.
- [17] I. Sari-Ali, B. Benyoucef, and B. Chikh-Bled, "Etude de la jonction PN d'un semi-conducteur à l'équilibre thermodynamique," *Journal of Electron Devices*, vol. 5, pp. 122-126, 2007.